# General analysis of receptor-mediated viral attachment to cell surfaces

T. J. Wickham,* R. R. Granados,‡ H. A. Wood,‡ D. A. Hammer,* and M. L. Shuler*
*School of Chemical Engineering, Cornell University, Ithaca, New York, 14853 and ‡Boyce-Thompson Institute for Plant Research, Cornell University, Ithaca, New York, 14853 USA

ABSTRACT Viruses are multivalent particles that attach to cells through one or more bonds between viral attachment proteins (VAP) and specific cellular receptors. Three modes of virus binding are presented that can explain the diversity in binding data observed among viruses. They are based on multivalency of attachment and spatial versus receptor saturation effects which are easily distinguished based upon simple criteria. Mode 1 involves only monovalent virus/receptor binding. Modes 2 and 3 involve multivalent bonds between the virus and cell; however, in mode 3 space on the cell surface becomes saturated before receptors.

A model is developed for viral attachment that accounts for nonspecific binding, receptor/virus interactions, and spatial saturation effects. The model can describe each mode in different limits and can be applied to virus binding data to extract key physical information such as receptor number and affinity. These values are used to postulate the type of VAP/receptor interaction involved and to predict binding at different parameter values. For the mode 2 binding of Adenovirus 2, the model predicts a receptor number of $4-15 \times 10^3$ on HeLa cells and an affinity of $2-6 \times 10^7\ M^{-1}$ which closely approximate experimental estimates. For the binding of three, broad-host-range, enveloped viruses, Semliki Forest virus, Vesicular Stomatitis virus, and the baculovirus, *Autographa californica* nuclear polyhedrosis virus, the model predicts receptor numbers of $10^5$ or greater and affinities in the range of $10^4$ to $10^5\ M^{-1}$. These values are indicative of a VAP/oligosaccharide interaction which has been documented for a number of other viruses. Experimental evidence is presented that is the first to demonstrate that baculovirus binding is mediated by a cell surface receptor.

## INTRODUCTION

Almost all viruses attach to the cell membrane via specific, saturable binding to cell surface receptors (Tardieu et al., 1982; Bukrinskaya, 1982). This binding reaction is mediated by virus attachment proteins (VAPs), present in multiple copies, which are unique to each virus type. The specificity and affinity of the VAP/cell receptor interaction contributes to the tissue specificity and host range of a virus and the expression of receptors on the cell surface has been strongly correlated with the susceptibility of the cell to infection (Tardieu et al., 1982; Maddon et al., 1986).

For many viruses their VAPs and respective receptors have been identified. The Human Immunodeficiency VAP is a 120-kD glycoprotein which binds to the CD4 receptor found on T cells (Dalgleish et al., 1984; Klatzman et al., 1984). Histocompatibility antigens have been identified as receptors for Semliki Forest virus (Helenius et al., 1978). Influenza viruses are well known to bind to sialyl-oligosaccharides on glycoproteins and glycolipids with the specificity of the interaction determined by the type of sialic acid linkage (Paulson et al., 1986). The Epstein-Barr virus binds specifically the complement receptor type 2 on B lymphocytes (Nemerow et al., 1986) and rhabdovirus has been shown to interact with the acetylcholine receptor (Lentz et al., 1982). The reovirus receptor is similar or identical to the mammalian beta-adrenergic receptor (Co et al., 1986) while encephalomyocarditis virus attachment is mediated by glycophorin A (Allaway et al., 1986). For viruses whose receptors have not been identified, it has been possible to demonstrate receptor-mediated attachment through three standard criteria (Tardieu et al., 1982): (*a*) Saturability. Virtually all viruses demonstrate a saturable binding component indicative of a discrete number of binding sites. (*b*) Specificity. Cells not expressing the specific virus binding component show no saturable binding. (*c*) Competition. Binding of radioactively labeled viruses can be blocked by unlabeled viruses or closely related viruses that share the same receptor.

Receptor-mediated viral binding is shared by nearly all viruses; however, the nature of the binding between different viruses appears diverse. A wide range of VAP's per virus and receptor types, affinities, and numbers exists. The number of VAP's per virus range from 12–60 for picornaviruses to up to 1,000 for some enveloped viruses. The Semliki Forest virus spike protein has a measured receptor affinity of $<6 \times 10^6\ M^{-1}$ and receptor

Address correspondence to Dr. Hammer.

number of at least $10^6$ per BHK-21 cell (Fries and Helenius, 1979). The gp120/CD4 affinity for Human Immunodeficiency virus (HIV) has been measured to be $2 \times 10^8$ $M^{-1}$ with a receptor number of $3 \times 10^3$ per murine hybridoma cell (Lamarre et al., 1989).

Whether a virus has a broad or narrow host range seems to correlate with the VAP/receptor interaction it uses (Marsh and Helenius, 1989). The binding of broad host range viruses is characterized by the binding of a common molecule or moiety on the cell. Influenza virus exemplifies this type by binding sialic acid moieties (Weis et al., 1988). The specificity of the binding properties of influenza viruses results from their differential interaction with the various types of sialic acid-containing carbohydrate structures present on glycoproteins or glycolipids (Paulson et al., 1986). Viruses such as paramyxoviruses and influenza viruses tend to bind in this manner. Narrow host range viruses are characterized by a high affinity bond with a specific protein. Rhinoviruses, polioviruses, and HIV have narrow host ranges and have been shown to bind to specific molecules that are part of the immunoglobin superfamily (White and Littman, 1989).

Scatchard analysis has typically been used to analyze virus binding; however, interpretations of the Scatchard curves in terms of quantities such as receptor number, VAP number, and receptor/VAP affinity is not straightforward. At least nine types of viruses have been analyzed by Scatchard analysis, which include Cytomegalovirus (Taylor and Cooper, 1989), Semliki Forest virus (Fries and Helenius, 1979), Vesicular Stomatitis virus (Schlegel et al., 1982), Rabies virus (Wunner et al., 1984), African Swine Fever virus (Alcami et al., 1989), Rhinovirus (Colonno et al., 1988), Adenovirus (Persson et al., 1983), Reovirus (Epstein et al., 1984), and Foot-and-Mouth Disease virus (Baxt and Morgan, 1986). Much of the virus attachment data conforms to this type of analysis in that a straight line can be drawn through the data to yield a virus affinity and site number. The site number obtained from these analyses provides insight into the mechanism of binding when compared with the receptor number that is separately measured. Not all viruses appear to bind in the same manner. Different binding modes should not be surprising given the diverse values of VAP number, receptor number, and receptor affinity that exist for viruses. The number of receptors for rhinovirus roughly equals the number of receptor antibody sites (J. Greve, personal communication), suggesting that only one receptor binds per virus. For many other viruses the receptor number is 10 to 500 times the virus site number, suggesting multivalent binding is involved. In some of these cases, space on the cell for the virus to bind appears to become saturated before the receptors because the virus site number (roughly 10,000–100,000 sites/cell) corresponds to a cell fully covered by viruses. Other viruses show from ~500–5,000 sites in which receptors become saturated before space becomes a limiting factor to further binding. Clearly, different modes of virus binding exist that are not directly apparent from the Scatchard analysis alone.

Thus, although receptor-mediated virus attachment is well accepted, a comprehensive, quantitative understanding of viral attachment is still lacking. The multivalency of a virus allows it to potentially form multiple bonds with cellular receptors. However, the steric availability of the VAP's and the receptor density, number, and affinity will affect the multivalency of the binding. For instance, low receptor density and/or steric unavailability of other VAP's after the binding of a virus to a single receptor will prevent the formation of multivalent bonds. The Scatchard analysis in this case would show zero cooperativity and a virus site number equal to the receptor number. At very high receptor densities, multivalent binding may occur but receptors may not be saturated because space on the cell surface becomes saturated before the receptors (results to be shown for a baculovirus). The number of sites would correspond to the maximum number of viruses that can fit onto the cell and the affinity would not correspond directly to the receptor affinity. At intermediate receptor densities multivalent binding and saturation of receptors would be possible, which would result in an apparent negative cooperativity as seen for other multivalent ligands. Thus, an understanding of the parameters that influence attachment, such as receptor number and density, virus concentration, and VAP/receptor affinity, is necessary to predict binding and how different modes of binding can occur.

The goal of this paper is firstly to propose three modes of receptor-mediated virus attachment that can account for the wide variety of published data and show how all of these modes include receptor-mediated attachment. Secondly, a tractable mathematical model is proposed that can elucidate the role of factors such as VAP/receptor affinity, receptor number and density, VAP number, and virus concentration on the overall binding, for each mode of binding. Because the gross appearance of binding between virus and cell is different in each of the modes, the model, in conjunction with experiment, indicates which mode of binding is operative in each system. This method will be shown to be applicable to a wide range of virus/cell systems, and it is expected to be useful in elucidating quantitative information about the key chemical and physical interactions which are involved in viral attachment. This work is the first to place explicit receptor information into a model for viral attachment.

Often, treatment of viral attachment has involved a mass action kinetic approach. The aggregation of small particles to large particles has been studied assuming single adhesion events to equivalent binding sites (Perelson, 1985; Brendel and Perelson, 1987). Other treatments

have studied the kinetics of both adhesion and fusion of virus particles to cells (Bentz et al., 1988; Tsao and Huang, 1986; Nir et al., 1986; Kuroda et al., 1985). These approaches usually involve a single-step reversible or irreversible attachment to binding sites, distinct from receptors, that are initially available and depleted during the course of binding. However, many viruses are thought to bind receptors multivalently, which would necessitate the inclusion of multiple, receptor-binding steps to accurately represent the attachment. Thus, the role of receptors in determining the overall forward and reverse attachment rates in the above approaches is not explicitly addressed.

The multivalent attachment of antigens where receptors are explicitly taken into account has been previously modeled (Macken and Perelson, 1982; Perelson, 1981; DeLisi, 1980*b*; Perelson and DeLisi, 1980; Gandolfi et al., 1978). However, because significant differences exist between viruses and multivalent antigens, an extension of this work is necessary to apply it to viral binding. Because a virus is conceived as a large, highly multivalent antigen, many aspects from these models have been borrowed. The neglect of complicated processes such as endocytosis and fusion makes such explicit consideration of receptors possible. Experimentally, these processes are eliminated by performing experiments at 4°C. The model provides an extremely useful and simple method for characterizing viral binding behavior and should be helpful to those studying viral processes in which viral attachment is important.

## PROPOSED MODES OF VIRUS ATTACHMENT TO CELLS

Three modes of receptor-mediated binding are proposed that differ with respect to the multivalency of attachment and the saturability of receptors and/or space on the cell. All the modes can be interpreted from the appearance of the virus Scatchard plot in relation to the Scatchard plot determined for the purified attachment protein. The modes are described in terms of the supporting experimental evidence, the expected appearance of the virus Scatchard plot, and roughly in the order of increasing complexity of the interactions involved.

### Mode 1: monovalent attachment

Mode 1 is simply the monovalent attachment of the virus to the cell (Fig. 1 *a*). This may occur because the virus is sterically unable to bind additional receptors or because a very low receptor density favors the formation of only a single bond. In this case, the Scatchard plot would be a

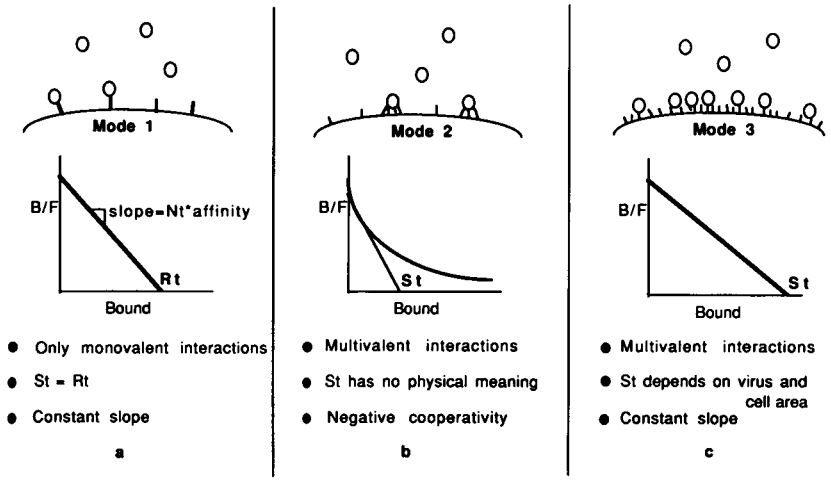


FIGURE 1 (*a*) Schematic of mode 1 attachment, the conditions under which it occurs, and the expected appearance of the Scatchard plot. Attachment is monovalent so that the number of virus sites, $S_t$, in the Scatchard plot is equal the number of receptor sites, $R_t$. The overall virus affinity is equal to the VAP affinity, $K_f'''$, multiplied by the total number of VAPs on the virus, $N_t$. (*b*) Schematic of mode 2 attachment, the conditions under which it occurs, and the expected appearance of the Scatchard plot. Attachment is multivalent so the apparent number of virus sites, $S_t$, is less than the number of receptors, $R_t$. The multivalency of attachment results in an apparent negative cooperativity as evidence by the continually decreasing slope of the plot as more viruses bind. (*c*) Schematic of mode 3 attachment, the conditions under which it occurs, and the expected appearance of the Scatchard plot. Attachment is multivalent, as for mode 2. Unlike mode 2, the space on the surface of the cell becomes saturated before the receptors, so that the number of virus sites, $S_t$, is determined by the projected virus area, $A_v$, and the virus exposed cell area, $A_c$. Because receptors are not appreciably saturated the overall affinity remains constant as evidenced by the constant slope. Intermediate regions between modes 2 and 3 are possible where both spacial and receptor saturation occur simultaneously.

straight line with the virus site number equal to the receptor number. The viral affinity would be expected to be $N_t$-fold greater than the individual VAP/receptor affinity, where $N_t$ is the number of VAP's per virus. The reversible binding of rhinovirus (Colonno et al., 1988) seems to fit this mechanism.

### Mode 2: receptor saturation with multivalent binding

This mode is the classically described mechanism of virus attachment. A virus first attaches to a single receptor followed by a series of reversible, receptor binding reactions (Fig. 1 *b*). Negative cooperativity is apparent in the overall binding which is to be expected for multivalent attachment. However, this apparent negative cooperativity must be interpreted with care. Other mechanisms, such as monovalent binding combined with nonspecific binding or two distinct binding sites, can show apparent negative cooperativity. The strongest evidence for multivalent binding comes from the separate measurement of receptor number using purified viral adhesion protein and comparison to the number of virus binding sites determined from Scatchard analysis. In this mode, the virus site number is smaller than the separately measured receptor number for many viruses. For example, HeLa cells have ~6,000 Adenovirus 2 receptors (Svensson, 1985) and ~2,000 Adenovirus binding sites (Persson et al., 1983). The overall affinity of the virus for the cell compared with receptor/VAP affinity presumably comes from multiple copies of VAP per virus that increase its forward attachment rate (as for mode 1) and are responsible for the multivalent binding of receptors.

### Mode 3: spatial saturation with multivalent binding

Mode 3 shares many characteristics with mode 2 except that both space and receptor saturation occur simultaneously (Fig. 1 *c*). Cells that contain very high numbers of viral receptors can become completely covered with virus before the receptors become saturated. Thus, the virus site number is determined by the ratio of cell area to the projected virus area. If only a small fraction of receptors are bound at full virus coverage the Scatchard plot would appear as a straight line even though multivalent binding is present. The overall virus affinity would be a function of the receptor density and affinity. Semliki Forest virus, Vesicular Stomatitis virus, and a baculovirus appear to attach by this mode. Also, it is likely that many other viruses that bind a common molecule or moiety could attach in this manner.

A final mode that has been proposed (Lipkind and Urbakh, 1988), but not observed experimentally, is domain binding. By this mechanism, the virus binds exclusively to a specific region of the cell, such as a coated pit. Because no direct evidence exists for a virus attaching only to coated pits domain attachment is not considered as a major mode of attachment and will not be included in this analysis. However, it is recognized that it could exist for some viruses.

## MODEL OF RECEPTOR-MEDIATED ATTACHMENT OF VIRUSES

### Mode 1

This mode is the case where each virus binds to a single receptor, and will appear as a straight line on a Scatchard plot (in a Scatchard plot bound/free is plotted against bound). An $N_t$-valent virus, $F$, attaches reversibly to a monovalent cellular receptor, $R_f$, to go to the bound state, $B$, with forward and reverse rate constants, $k_f'''$ and $k_r$, respectively. The rate constant $k_f'''$ is used to distinguish a forward reaction that occurs from the bulk from one that could occur after the virus is on the surface, represented by $k_f''$ (the superscript, ''', refers to three dimensional binding, and, '', refers to surface binding). At equilibrium

$$\frac{B}{F} = N_t \cdot K_f''' \cdot (B + R_t), \tag{1}$$

where $R_t$ is the total receptor number and $K_f'''$ is $k_f'''/k_r$. In mode 1, additional cross-linking (multivalent) interactions do not occur because of steric factors or because receptor density is very low. The mathematical solution is the same as would be for a monovalent/monovalent ligand/receptor interaction except that the forward binding rate is $N_t$-fold higher than for a monovalent VAP binding reaction. Thus, the overall virus affinity will be $N_t$-fold larger than the VAP/receptor affinity and the receptor number will equal the virus site number (Fig. 1 *a*).

### Mode 2

Modeling this mode follows the formalisms previously developed (Gandolfi, 1978; Perelson, 1981) that were used to analyze the attachment of multivalent ligands. Only a minor modification is made to include a binding state that accounts for the nonspecific binding that nearly all viruses exhibit, particularly those such as Vesicular Stomatitis virus and closely related viruses (Schlegel et al., 1982). Thus, except for the nonspecific binding, the rate and equilibrium equations are given by Perelson (1981) and will not be developed here. Only the pertinent equilibrium solutions will be presented, with the minor modification of nonspecific adsorption included.

A schematic of the model is shown in Fig. 2. Viruses first reversibly diffuse to the cell surface where they may undergo a series of discrete, reversible reactions with viral receptors. The ultimate number of these reactions per virus, $N$, is limited by the number of VAPs per virus and their accessibility to viral receptors. The virus population, $F$, first binds to one receptor with the rate constant, $k_f'''$. After binding one receptor, the virus in the $B_1$ state can proceed to the $B_2$ state with a rate constant, $k_f''$. A virus particle can continue to bind receptors with a rate constant, $k_f''$, up to the $B_N$ state where all of its potential binding sites are occupied by receptors. A virus with $n$ bound receptors may experience a dissociation reaction with the rate constant, $k_r$, and enter the $n$-1 bound state. Viruses may also nonspecifically attach to the cell surface without the involvement of receptors. Nonspecific attachment is an experimentally measurable quantity (Epstein et al., 1984; Schlegel et al., 1982); however, it may not be possible to distinguish virus/cell from virus/virus nonspecific attachment when many viruses attach (see Appendix, A-1). Unbound viruses, $F$, bind nonspecifically to become, $L$, with a forward rate constant, $k_{+1}$, and a reverse rate constant, $k_{-1}$. No receptors are lost in this reaction. The nonspecific binding is only a minor factor in the modeling but can be an important effect to consider when applying the model to experimental data (see Appendix, Fig. A-1).

The VAP/receptor interaction is assumed monovalent with only one type of viral receptor. Only diffusional transport of the virus to the cell surface is considered and effects such as convective transport (bulk flow) are not included. Also, fluid and thermal forces which might affect the dissociation reactions of viruses in the lower-bound states are not taken into account. The cross-linking constants, $k_f''$ and $k_r$, are assumed to be constant for all the cross-linking reactions and thus represent average two-dimensional forward and reverse reaction rates.

Rate equations can be written for each of the steps according to mass action kinetics (Perelson, 1981). The constants and variables are outlined in Table 1. With the individual rate constants and initial conditions these equations can be solved numerically to provide simulations of virus particle binding over time. For application to equilibrium virus binding, the equations may also be solved by setting the rates to zero (Perelson, 1981). The equilibrium solution yields a set of recursive relations. The pertinent solutions, including nonspecific adsorption, are shown below.

The virus conservation equation is the sum of all the virus populations:

$$f_o = f + l + \sum_1^N b_n. \tag{2}$$

The receptor balance is obtained from the summation of the free receptor population and all the bound receptors in states 1 to $N$:

$$r_o = r_f + \sum_1^N n \cdot b_n. \tag{3}$$

A set of recursive relations are obtained for the population of viruses that are bound by $n$ receptors. For viruses bound

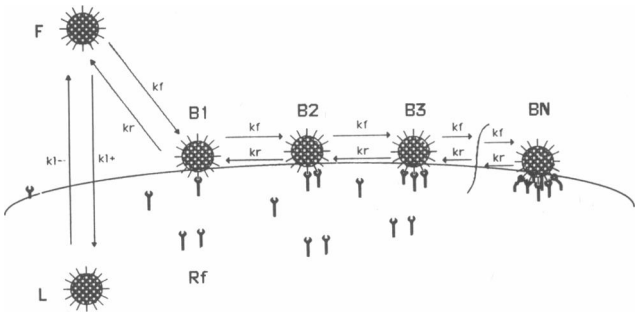


FIGURE 2 Schematic of the model for virus attachment to cells. Virus in the $F$ state may reversibly attach nonspecifically in the state, $L$, with forward and reverse rate constants $k_{1+}$ and $k_{1-}$. This step does not bind any receptors. Virus in the $F$ state may also reversibly bind a receptor to go to the $B_1$ state with forward and reverse rate constants $k_f'''$ and $k_r$. Viruses from the first state to the $N$-1 state may reversibly bind to or dissociate from a receptor to go the state immediately above or below. All the receptor cross-linking reactions are assumed to have the same forward and reverse rate constants $k_f''$ and $k_r$. Viruses in the state $B_N$ may only dissociate from a receptor. $N$ represents the maximal number of virus attachment proteins that can be bound per virus particle.

**TABLE 1 Dimensionless variables and constants used in the model**

| Dimensionless variables | |
|---|---|
| $f = \frac{F}{F_o}$ | $b_n = \frac{B_n}{F_o}$ |
| $l = \frac{L}{F_o}$ | $r_f = \frac{R_f}{R_{fo}}$ |
| **Dimensionless equilibrium constants** | |
| $R_v = \frac{F_o}{R_{fo}}$ | $\sigma = \left(\frac{N_t}{N}\right) \cdot \left(\frac{K_f'''}{K_f''}\right)$ |
| $K_r = \frac{k_f''}{k_r} \cdot R_{fo} = K_f'' \cdot R_{fo}$ | $K_1 = \frac{k_{1+}}{k_{1-}}$ |

The dimensional receptor and virus populations $R_{fo}$, $F_o$, and $B_n$ are all expressed in number per unit area of cell. The dimensionless variables are: unbound nonsurface associated virus, $f$; surface associated virus in the bound state, $n$, is $b_n$; nonspecifically bound virus, $l$; unbound receptors, $r_f$. The equilibrium constants are: the ratio of total viruses to the total receptors, $R_v$; cross-linking, $K_r$; nonspecific binding, $K_1$.

by one receptor,

$$b_1 = N_t \cdot (K_f''' \cdot R_{fo}) \cdot f \cdot r_f. \quad (4)$$

For the nonspecifically bound viruses,

$$l = K_l \cdot f. \quad (5)$$

For the viruses bound by $n$ receptors,

$$b_n = K_r \cdot \frac{(N - n + 1)}{n} \cdot b_{n-1} \cdot r_f, \quad (6)$$

where $K_r = K_f'' \cdot R_{fo}$.

And thus, the total number of receptor-bound viruses is

$$\sum_1^N b_n = \sigma \cdot f \cdot \sum_1^N \left[ (K_r \cdot r_f)^n \cdot \prod_1^n a(n) \right], \quad (7)$$

where

$$a(n) = \frac{(N - n + 1)}{n} \quad \text{and} \quad \sigma = \left(\frac{N_t}{N}\right) \cdot \left(\frac{K_f'''}{K_f''}\right).$$

The unbound virus is given by

$$f = \left\{ 1 + K_l + \sigma \cdot \sum_1^N \left[ (K_r \cdot r_f)^n \cdot \prod_1^n a(n) \right] \right\}^{-1}. \quad (8)$$

Using the receptor balance given by Eq. 3 the unbound receptor concentration becomes

$$r_f = 1 - R_v \cdot \sigma \cdot f \cdot \sum_1^N \left[ n \cdot (K_r \cdot r_f)^n \cdot \prod_1^n a(n) \right], \quad (9)$$

where $R_v = F_0/R_{f0}$.

Substituting the relation in Eq. 8 into Eq. 9, an implicit solution for the unbound receptor concentration, $r_f$, is obtained

$$r_f = 1 - \left\{ \frac{R_v \cdot \sigma \cdot \sum_1^N \left[ n \cdot (K_r \cdot r_f)^n \cdot \prod_1^n a(n) \right]}{1 + K_l + \sigma \sum_1^N \left[ (K_r \cdot r_f)^n \cdot \prod_1^n a(n) \right]} \right\}. \quad (10)$$

Eq. 10 can be solved by standard numerical techniques such as the Newton-Raphson method. Solutions for all the other populations is then obtained from the recursive relations given by Eqs. 5–8. Thus, the equilibrium solution requires the knowledge of the total virus concentration, $F_0$, the nonspecific virus/cell affinity, $K_l$, the cross-linking affinity, $K_f''$, the total receptor density, $R_{fo}$, the three-dimensional affinity $K_f'''$, and the number of accessible VAP molecules per virus, $N$. It is well known $K_f'''$ and $K_f''$ are not independent; one can be calculated from the other (Bell, 1978).

The numerical approach used to solve both the kinetic and equilibrium problems is different from the analytical solutions of Perelson (1981) which can handle the special cases of multivalent ligand attachment to low valency multivalent receptors. However, in the Perelson solution the total ligand concentration was assumed to be equal to the unbound ligand concentration (i.e., ligand is not limiting) which is not usually a good assumption for viruses at physiological concentrations. For example, in a typical binding experiment more than half of the total virus particles may be bound. For the case of a multivalent virus attaching to monovalent receptors we were able to solve the kinetic and equilibrium problems for viruses by standard numerical techniques (Hindmarsh, 1983; Press et al., 1983).

## Mode 3

This mode shares all the complexities of model 2 with the additional factor of spatial saturation. The forward attachment rate becomes proportional to the amount of free attachment space as viruses bind and space becomes saturated. The amount of free attachment space is simply described in terms of the cell area and the number of bound viruses. Thus, for mode 3, the three-dimensional forward attachment rate constant, $k_{f3}'''$, can be represented as a function of the bound virus concentration

$$k_{f3}''' = \left[ 1 - \frac{(A_v \cdot \Sigma b_n)}{A_c} \right] \cdot k_f''', \quad (11)$$

where $A_v$ is the projected area of the virus, $A_c$ is the area of the cell, and $\Sigma b_n$ is the number of bound virus per cell. The forward rate constant when no viruses are bound, $k_f'''$, is the same forward constant as in mode 2. The two-dimensional rate constant, $k_f''$, is unaffected by spatial saturation and remains the same in modes 2 and 3.

### Defining the relationship between $K_f'''$ and $K_f''$

An important feature of modeling the multivalent attachment of viruses is the relation between the three-dimensional equilibrium constant, $K_f'''$ ($k_f'''/k_r$), for the initial receptor/virus interaction and the two-dimensional constant for the cell surface cross-linking reactions, $K_f''$ ($k_f''/k_r$), given by the parameter, $\sigma$, in Eqs. 7–10. Reversible, receptor-binding reactions are typically represented as a reversible transport step and a reversible reaction step (Eigen, 1974; DeLisi, 1980*a*). Using Smoluchowski theory (Smoluchowski, 1917), the transport step, with forward and reverse rate constants $k_+$ and $k_-$, involves the diffusion of the ligand to and away from the region where it is capable of binding. Once the ligand is within this region, it is capable of binding with forward and reverse reaction rate constants $k_{+1}$ and $k_{-1}$. In terms of these constants, the equilibrium constant, $K_f'''$, is the product of the transport and reaction equilibrium con-

stants which themselves are the ratios of their respective forward and reverse rate constants

$$K_f''' = \left(\frac{k_+}{k_-}\right)''' \cdot \left(\frac{k_{-1}}{k_{-1}}\right)'''. \quad (12)$$

When relating $K_f'''$ and $K_f''$, the inherent reaction step for the VAP/receptor bond remains the same; thus,

$$\left(\frac{k_{+1}}{k_{-1}}\right)''' = \left(\frac{k_{+1}}{k_{-1}}\right)''. \quad (13)$$

The three-dimensional transport equilibrium constant is given by:

$$\left(\frac{k_+}{k_-}\right)''' = \frac{4}{3} \cdot \Pi \cdot s^3, \quad (14)$$

where $s$ represents the radius defining the region where reaction becomes possible.

For purely two-dimensional transport in Smoluchowski theory, the corresponding equilibrium constant is given by:

$$\left(\frac{k_+}{k_-}\right)'' = \Pi \cdot s^2. \quad (15)$$

These expressions (Eqs. 12–15) allow the relation of the two equilibrium constants, $K_f'''$ and $K_f''$, that are contained in the factor, $\sigma$, in Eqs. 7 to 10 for the case where virus binding is considered as three-dimensional diffusion and reaction followed by purely two-dimensional diffusion and cross-linking reactions

$$\sigma = \left(\frac{N_t}{N}\right) \cdot \left(\frac{4}{3}\right) \cdot s. \quad (16)$$

Thus, after a virus binds one receptor, all the variable VAP's are considered to be in the proper plane of orientation for two-dimensional diffusion and reaction with receptors to occur. Provided this assumption is valid, it is then possible to apply the model to equilibrium virus binding data. Values of $K_f'''$ and $R_{fo}$ can be obtained, given estimates of $N_t$, $N$, and $s$.

The above relation is likely an oversimplification for virus attachment. It relies on the assumption that all the available VAP's lie in the proper plane and orientation after the first bond formation. Geometrical considerations for a virus at a cell surface clearly demonstrate that the major assumption in Eq. 16 involving VAP orientation is not correct. Fig. 3 shows the spatial relationships for Semliki Forest virus, given known lengths and numbers for the VAP (Fries and Helenius, 1979), after binding one receptor, with a typical value for $s$. Clearly, the closest VAP's to the bond are not always in the proper plane to react. VAP's farther away from the bond are much less likely to be in the proper plane.

Consequently, the relation between $K_f'''$ and $K_f''$ is not as simple as Eq. 16. An accurate relation between the two constants would require a knowledge of the statistical thermodynamic distribution functions for the VAP and receptor, which include spatial as well as orientational factors (Crothers and Metzger, 1972). Obtaining these functions requires the known values of VAP number, length, and orientation. However, more importantly, the functions also require unknown or hard to calculate quantities, such as VAP and receptor flexibility, membrane fluctuations, charge effects, and steric effects due to other proteins on the membrane. Additionally, the distribution functions would change as a function of the number of bonds formed.

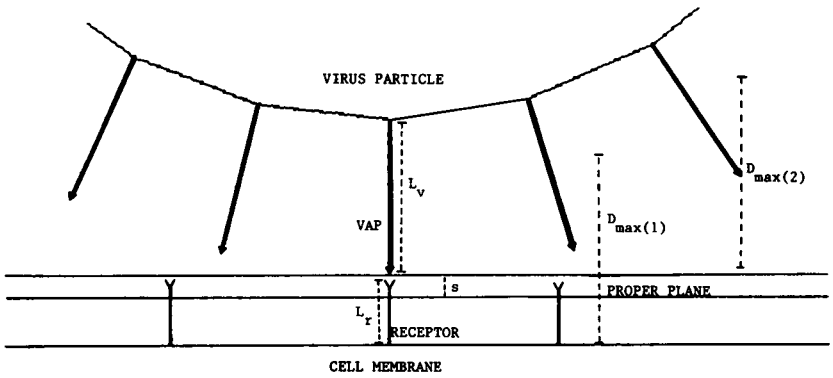


FIGURE 3 Close-up schematic of Semliki Forest virus binding based upon the reported values for VAP number, $N_t$ (250), and length, $l_v$ (8 nm), (Fries and Helenius, 1979) and estimated values for receptor length, $l_r$, (4 nm) and the interaction distance at which a bond may form, $s$ (1 nm). This information can be used to predict an upper limit on the probability, $P$, that can be approximated as $s/D_{(max)1}$, where $D_{(max)}$ is the vertical range from the cell membrane that a VAP may traverse. Thus, it is seen that the six nearest neighbors to the initial bond react according to the probability determined by $D_{(max)1}$ while the next ring of neighbors is much less likely to react because $D_{(max)2}$ does not intersect the plane of reaction.

The complexity of the interactions combined with the imprecise knowledge of many of the factors makes the use of intricate distribution functions for each reaction impractical. In keeping with the simplicity of the model and to keep it tractable, a probability factor was introduced into Eq. 16. The factor, $P$, represents the probability that an unbound VAP will be in the proper plane and orientation to react. A modification of Eq. 16, the relationship between $K_f'''$ and $K_f''$, which takes into account the expected reduction in the cross-linking rate due to restricted access of receptor for VAP after the first binding step, is

$$K_f''' = K_f'' \cdot \left(\frac{4}{3}\right) \cdot \left(\frac{s}{P}\right). \quad (17)$$

The assumption of an average $K_f''$ for all the cross-linking steps is maintained. Also, the ratio of three- to two-dimensional reaction rates, $\sigma$, becomes

$$\sigma = \left(\frac{N_t}{N}\right) \cdot \left(\frac{4}{3}\right) \cdot \left(\frac{s}{P}\right). \quad (18)$$

The obvious drawback of using this factor is that it adds an additional parameter to the model arising from the insufficient knowledge of the relation between $K_f'''$ and $K_f''$. However, the probability factor, $P$, can be roughly calculated based on geometrical considerations. It is similar to a distribution function that would more precisely describe the interaction since both would essentially include the probability that a ligand is in the proper space and orientation to react. Provided one can estimate $P$ a priori, this value can be used in the model when applied to experimental data to obtain quantitative information abount fundamental constants involved in virus attachment, such as $K_f'''$ and $R_{fo}$. Alternatively, if $K_f'''$ and $R_{fo}$ have been separately determined, the value of $P$ can be determined from data and compared with its estimated value. Also, once determined, the value of $P$ would be expected to remain constant for a given virus under a variety of conditions because it depends mainly on the geometry of the virus, adhesion protein, and receptor which do not change between binding experiments.

## RESULTS

### Demonstration of spatial saturation for a baculovirus

Baculoviruses are a group of enveloped viruses that infect insect hosts and are in widespread use as a vector for recombinant protein production. Their route of infection and general method of replication is virtually identical to many other mammalian viruses so that it is expected that their attachment is also biophysically similar to other mammalian viruses. In fact, some viruses, such as Vesicular Stomatitis virus, are capable of infecting mammalian or insect host cells.

Binding experiments with the baculovirus, *Autographa californica* multiple nuclear polyhedrosis virus (AcMNPV), demonstrate that spatial saturation occurs. Also, after space on the cell is saturated, virus/virus binding predominates which is not spatially limited (virus can adsorb in multilayers). Experiments were performed in wells using confluent attached cells, where the area of the well closely corresponds to the exposed area of the confluent monolayer (see Appendix, A-4 for details of procedures). The Scatchard plot for AcMNPV binding to *Spodoptera frugiperda*-9 (Sf-9) cells is shown in Fig. 4 *a*. The total number of virus particles bound per well at saturation was virtually constant, independent of which of five cell types were used or whether cells were even present (bare well) (results not shown). When binding to bare wells, the area per binding site was identical to the laterally projected area of a baculovirus particle. Also, each exhibited nearly the same percentage of binding beyond the point where space was saturated. Continued binding beyond the maximum number of virus/cell sites indicates the degree of virus/virus binding (see Appendix, A-1). The Scatchard plots for Vesicular Stomatitis virus (VSV) (Fig. 4 *b*) and Semliki Forest virus (SFV) (Fig. 4 *c*) show that they probably attach by mode 3, in a fashion similar to that of baculovirus binding to *Spodoptera frugiperda*-9 insect cells (Fig. 4 *a*).

### Estimation of affinity and receptor number using the model

Based on the Scatchard plot and the size of the virus and cell it is immediately possible to distinguish mode 3 from the other modes. In mode 3, the number of sites determined will be equivalent to the maximum number of viruses that can fit onto the cell surface. For viruses that do not exhibit spatially limited binding (modes 1 and 2) it is necessary to compare the virus site number, $S_T$, with the virus receptor number, $R_T$, determined separately using purified VAP or an antibody to the receptor. Mode 1 corresponds to $S_T = R_T$, and that either $P = 0$ and/or $N = 1$. For rhinovirus, the rough equivalence of the number of virus sites and receptor antibody sites (J. Greve, personal communication) suggests that it binds monovalently by mode 1 (Fig. 5). For Adenovirus however, $R_T$ is greater than $S_T$ and shows negatively cooperative binding (Svensson, 1985; Persson et al., 1983). Thus, adenovirus appears to bind multivalently by mode 2 (Fig. 6).

Receptor number and affinity ranges could be estimated by fitting the model to experimental binding data.

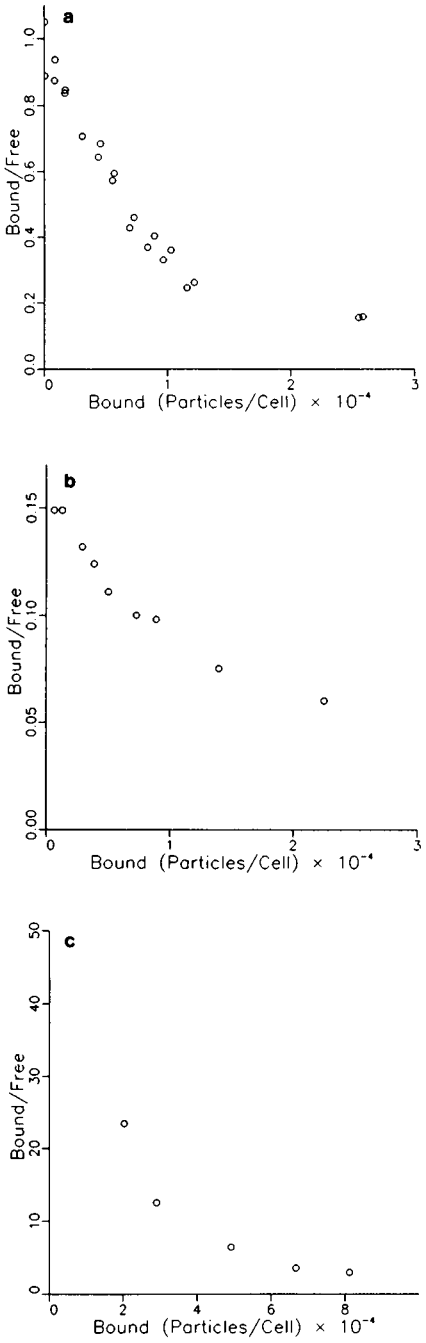


FIGURE 4 (*a*) The Scatchard plot for the baculovirus, *Autographa californica* Multiple Nuclear Polyhedrosis virus attaching to *Spodoptera frugiperda*-9 cells. Virus/virus binding was measured to be 5–10% of input when the cell was fully covered by virus. Experimental protocol is given in the Appendix. (*b*) The Scatchard plot for the published binding data of Vesicular Stomatitis virus attaching to Vero cells (Schlegel et al., 1982). The specific and nonspecific binding were both measured. (*c*) The Scatchard plot for the published binding data of Semliki Forest virus attaching to BHK-21 cells (Fries and Helenius, 1979). Nonspecific binding was not measured but could be estimated as was done for Adenovirus (see Figure 6, caption).

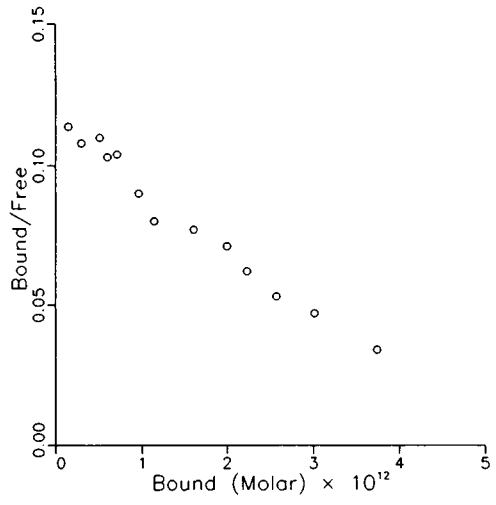


FIGURE 5 Data for the attachment of rhinovirus to HeLa cells. The bound virus concentration is given in molar so that the overall virus affinity can be estimated directly from the plot (Colonno et al., 1988).

Fits were acceptable if they fell within a preset mean error, which was the sum of the absolute differences between the data and the model divided by the total number of data points. For AcMNPV the average error of 11 duplicate data points was 2% (Fig. 4 *a*) (for experimental protocol see Appendix, A-4). The cut-off for acceptable parameter values was determined from fits that fell within 3% mean error of the data. Error bars were not reported for the other virus binding data so mean error

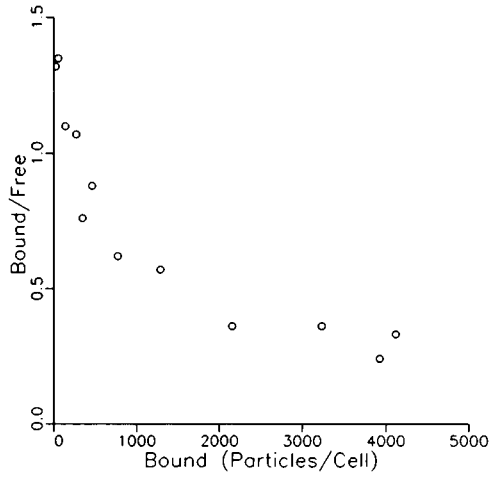


FIGURE 6 Data for the attachment of Adenovirus 2 to HeLa cells in suspension at 4° C (Persson et al., 1983). For this system the nonspecific binding was not directly measured but was estimated from the region of the curve where the data flattened out, where nonspecific virus/cell binding dominates.

cutoffs were chosen to be 2–3% above the mean error of a best fit line through the data. An 8% mean error cut-off was used for Adenovirus (Fig. 6) and a 4% mean error cut-off was used for VSV (Fig. 4 *b*) and SFV (Fig. 4 *c*). The Scatchard plots for each virus were obtained directly from the literature and converted, when necessary, to the form shown using the reported cell concentrations (Figs. 4, *a–c* to Fig. 6).

## Mode 1: rhinovirus

The model is applied to rhinovirus 14 binding to HeLa cells (Colonno et al., 1988) according to mode 1. A gross simplification of Eqs. 2–10 results when $P = 0$ and $N = 1$, so that Eq. 1 can be used. For rhinovirus $N_t = 60$ so that $K_{aff(VAP)} = K_{aff(virus)}/N_t$ and $S_T = R_T$. Thus, for the data in Fig. 5 the receptor number is 1,000–2,000/cell and the VAP affinity is $3.8 \times 10^8\ M^{-1}$, using the overall affinity from the slope, which is $2.3 \times 10^{10}\ M^{-1}$.

## Mode 2: adenovirus 2

Adenovirus is assumed to bind by mode 2 because the amount of Adenovirus which binds does not completely cover the cell surface, and the binding displays negative cooperatively. To fully specify the binding it is necessary to know $N_t$, $N$, $K_f'''$, $R_{fo}$, and $P$ in the model. As for the Scatchard analysis it is possible to estimate two constants by measuring binding as a function of different input virus concentrations and fitting the model to the data. For adenovirus $N_t$ is 12. $N$ is assumed to be 6 because after the first bond is formed the complex has five nearest neighbors. All other VAP's face away from the cell surface. The remaining constants are unknown; however, some of their values are known to exist within ranges. For example, the $x$-intercept of the Scatchard plot indicates that there are ~2,000 virus binding sites (Persson et al., 1983). Independent data indicates there are roughly 6,000 receptors (Svensson, 1985). Soluble attachment protein competes off 10 to 90% of attached viruses over a concentration range of $\sim 10^{-7}$ to $10^{-9}$ M (Philipson et al., 1968). The range of possible VAP affinities is thus taken to be $10^7$ to $10^9\ M^{-1}$. The probability factor, $P$, has an upper limit of ~0.03 (Appendix, A-2) and a lower limit of 0 (mode 1). By choosing different values of $P$ in a likely range of 0.001–0.03, it was possible to determine the ranges in receptor number and affinity that would fit the data within a mean error of 8% (Fig. 7). From this analysis, the model determined the receptor number and affinity range to be $0.4–1.5 \times 10^4$ receptors/cell and $1.0 \times 10^7$ to $1 \times 10^8\ M^{-1}$, respectively. Mode 1 binding, corresponding to $P = 0$, could not fit the data. The model predicts the affinity to be $2–6 \times 10^7\ M^{-1}$ using the independently determined receptor number of 6,000 (Fig. 7).

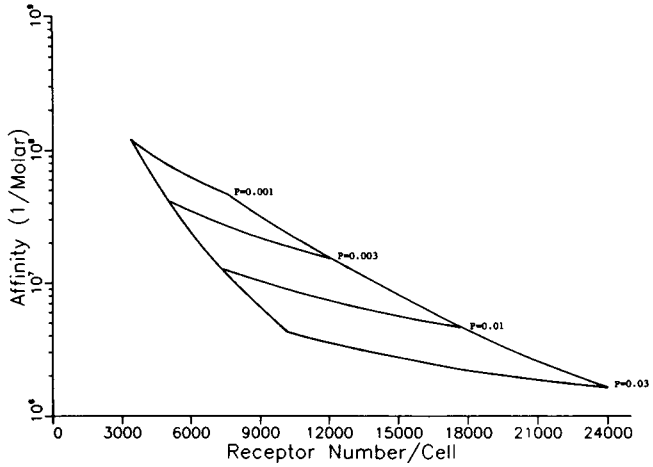


FIGURE 7 Parameter space for values of affinity and receptor number that fit the Adenovirus binding data in Fig. 6 for realistic values of $P$ (0.001–0.03) within a mean error of 8%. Using the experimentally determined receptor number, $R_{t(exp)}$, shows that the model predicts a VAP/receptor affinity of $2–6 \times 10^7\ M^{-1}$. The lower experimental estimate for the affinity, $10^7\ M^{-1}$, limits the receptor number range estimated by the model to $\sim 4–15 \times 10^3$/cell.

## Mode 3

For mode 2 the $B/F$ intercept and curvature of the plot allow the simultaneous and unique determination of receptor number and affinity for a given value of $P$, with the only variation arising from error in the data. In mode 3, however, the slope of the plot is not determined by receptor saturation but by spatial saturation. The spatial saturation masks any receptor saturation that would allow the simultaneous determination of receptor number and affinity. Instead of receptor number, one of the constants provided by the Scatchard analysis of mode 3 binding is the number of virus sites, $S_T$, which is determined by the size of virus and cell. Only one other constant can then be uniquely determined from the binding data, given the others are known.

## Baculovirus

Little is known about the attachment of baculovirus to insect cells. A 64-kD glycoprotein, present in large amounts on the virus envelope, has been implicated in attachment of the baculovirus, AcMNPV (Volkman, 1986). A protein receptor appears to exist for AcMNPV because pretreatment of cells with proteinase K reduces

binding by over 90% and because some cell lines do not saturably bind the virus (unpublished results).

For AcMNPV, $N_t$ was estimated to be ~1,000 and $N$ was taken to be 7 (Appendix, A-3). Even with three unknown parameters, $P$, $R_t$, and $K_f'''$, it was possible to establish limits on the affinity and receptor number that would fit the data. Fig. 8 *a* shows that for a given value of $P$ the relation between affinity and receptor number has a slope of 1, indicating that the lines of constant $P$ are also lines of constant $K_r$. Given $P$, $N_t$, and $N$, $K_r$ uniquely determines the $B/F$ intercept. The cutoff line extending from low to high affinities indicates the point where spatial saturation failed to dominate and receptor saturation introduced negative cooperativity into the plot. Past the cutoff line, along a line of constant $K_r$ and $P$, the $B/F$ intercept remains constant but the initial slope begins to change and is no longer determined by spatial factors alone.

The physical limit on receptor number is probably $\sim 10^7$, so that for a likely range of $P$, 0.001 to 0.1, the predicted AcMNPV receptor number on Sf-9 cells ranges from $10^5$ to $10^7$/cell (Fig. 8 *a*). The upper limit on affinity is $10^6$ $M^{-1}$, supporting the proposition that broad host range enveloped viruses attach via multiple, low affinity bonds (Marsh and Helenius, 1989; Marsh, 1984; Helenius and Marsh, 1982). A significant region of parameter space lies in the affinity range of $10^4$ to $10^5$ $M^{-1}$, which is a range commonly observed for lectin/sugar bonds (Hertz et al., 1985; Boldt and Lyons, 1979). Other enveloped viruses, notably the paramyxoviruses (Paulson et al., 1979; Haywood, 1974), influenza viruses (Paulson et al., 1986), polyoma virus (Cahan et al., 1983), and encephalomyocarditis virus (Burness, 1981) have been shown to bind via sialyloligosaccharide receptors. These results indicate that a sugar bond may be involved in AcMNPV attachment.

## Vesicular stomatitis virus

Receptor-mediated attachment of the rhabdovirus, VSV, has not been conclusively proven. The VAP for rhabdoviruses is believed to be G protein present at ~1,000 copies per virus (Schlegel et al., 1982). VSV, like many other enveloped viruses, displays two types of binding activity that are pH dependent. There is an acidic pH binding to phospholipids that is used by the virus to enter the cell once it has been internalized into the endosome. VSV strongly binds phosphatidylcholine or phosphatidylserine liposomes at acidic pH's (Yamada and Ohnishi, 1986). The second type of binding appears to be receptor-mediated and predominates at physiologic pH. It is used by the virus to initially attach to the cell so that it can be internalized. The receptor has not yet been identified for VSV, however, proteins do not appear to act as receptors. Trypsin pretreatment of cells increases the binding of the virus (Yamada and Ohnishi, 1986). Recent evidence indicates that the closely related rabies virus (also a rhabdovirus) binds glycolipids at physiological pH (Wunner et al., 1984). Using purified VAP a VSV receptor number of $3 \times 10^5$ was measured on BHK-21 cells (Thimmig et al., 1980).

As for baculovirus, the same type of analysis was done for VSV to determine regions of parameter space that could fit the data in Fig. 4 *b* (Fig. 8 *b*). Fig. 8 *b* is similar to Fig. 8 *a* but is shifted down in receptor number. It shows that the maximum affinity is $\sim 10^6$ $M^{-1}$ and, similar to AcMNPV, a significant region of acceptable parameter fits that lies between $10^4$ and $10^5$ $M^{-1}$ in affinity. If the receptor number determined for BHK-21 cells is used as the receptor number for Vero cells, the model predicts an affinity between $10^4$ and $10^5$ $M^{-1}$. An alternate possibility could be that the VAP interacts very weakly with lipids on the cell surface. As the affinity between receptor and VAP drops very low and the receptor number increases in the model, the concept of receptor-mediated attachment fades and is replaced by the idea of a nonspecific attachment to the cell membrane via very low-affinity interactions with membrane lipids. It is likely that both types of binding are present to some degree given the dual nature of VSV binding.

## Semiliki forest virus

Application of the model to SFV binding to BHK-21 cells (Fig. 4 *c*) to determine binding constants is shown in Fig. 8 *c*. There are ~250 copies of spike glycoproteins on the surface of SFV (Fries and Helenius, 1979). For the probability range of 0.1–0.001 the receptor numbers predicted by the model are $10^6$ or greater with affinities ranging from $\sim 10^4$–$10^6$ $M^{-1}$. Using purified octomeric VAP complex, cells could be completely covered (spatially saturated) with $\sim 10^6$ complexes per cell (Fries and Helenius, 1979). Therefore, BHK cells must possess at least $10^6$ receptors. In agreement with this independently determined result, the model also predicts that there are at least $10^6$ receptors/cell.

# DISCUSSION

The first purpose of this work is to propose reasonable modes of attachment that are based on simple observations, such as the relation between receptor number and viral site number, and the relation between virus size and $S_t$. These simple considerations can then be used as guidelines to quickly establish what mode is involved for a

given virus/cell system. Subtleties in binding, such as virus/virus binding and spatial saturation, are important factors to consider in interpreting binding curves. Neither of these factors has been previously recognized.

The second purpose of this work has been to provide a coherent mathematical model capable of predicting each of the binding modes and to apply the model toward the analysis of virus binding data. In applying the model to published binding data it has been necessary to extend the previous work by accounting for spatial and nonspecific binding effects, and to incorporate well-known relations between the first three-dimensional receptor interaction and the following two-dimensional receptor interactions (Eigen, 1974). The model is able to predict quantitatively the effects of factors that are expected to influence virus binding. Used as an analytical tool, the model allows the interpretation of equilibrium virus binding data in terms of more fundamental, relevant quantities, such as receptor number, receptor-ligand affinity, cell size, and VAP number.

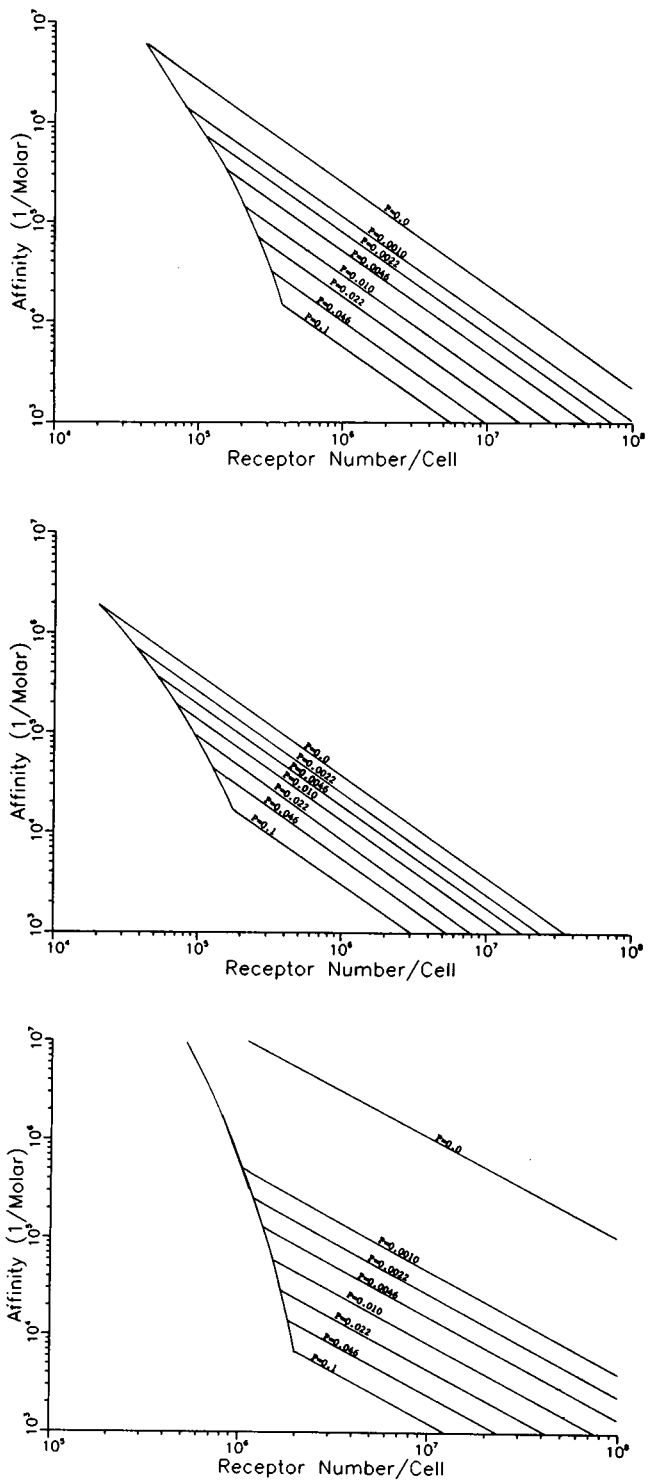


Modes 1 and 2 can be directly analyzed using the equilibrium solution of Perelson (1981). However, obtaining direct physical information from experimental data requires a faithful relation between the three-dimensional equilibrium constant and the two-dimensional cross-linking constant. Eq. 16 is one possible relation but it makes the drastic assumption that available VAP's are in the proper plane and orientation to bind according to the two-dimensional constant that describes the process. By simple geometrical considerations of virus attachment it has been shown that available VAP's are usually *not* in the proper plane to react. In fact, we have been able to show that using Eq. 16 which assumes that all VAP are in the proper plane to react ($P = 1$), we cannot describe much of the available virus binding data. Relationships have been developed using statistical mechanics to relate the two- and three-dimensional binding constants which take into account molecular orientation and have been used to predict antibody binding (Crothers and Metzger, 1972). However, this method would require a knowledge of the VAP and receptor distribution functions which are not easily estimated with the limited knowledge of their structure and dynamics. Consequently, the lumped parameter, $P$, has been introduced into Eq. 17 to account for the

FIGURE 8 (*a*) Parameter space for values of affinity, receptor number, and the factor, $P$, that fit the AcMNPV binding data in Fig. 4 *a* within a mean error of 3%. No experimental estimates of affinity or receptor number are available, however, the model predicts a receptor range from $10^5$ to an estimated physical limit of $10^7$/cell and affinities ranging from $10^3$ to $10^6$ $M^{-1}$ for realistic values for $P$ (0.001–0.1). (*b*) Parameter space for values of affinity, receptor number, and the factor, $P$, that fit the VSV binding data in Fig. 4 *b* within a mean error of 4%. The model predicts a receptor range of about $3 \times 10^4$ to $10^7$/cell and affinities ranging from $10^3$ to $10^6$ $M^{-1}$ for realistic values for $p$ (0.001–0.1). Using the receptor number measured by Thimmig et al. (1980) the model predicts an affinity of $10^4$–$10^5$ $M^{-1}$. (*c*) Parameter space for values of affinity, receptor number, and the factor, $P$, that fit the SFV binding data in Fig. 4 *c* within a mean error of 4%. The model predicts a receptor number of $10^6$–$10^7$ /cell and affinities ranging from $10^3$–$5 \times 10^5$ $M^{-1}$ for realistic values for $P$ (0.001–0.1).

average probability that an additional VAP is in the proper plane to react and to account for the possible effect of bond strain in increasing the reverse rate constant. This approach is related to the statistical mechanic approach in that both consider a probability of the VAP being in the proper position and orientation to react.

Previous work (Bentz et al., 1988; Nir et al., 1986) has modeled the attachment kinetics of Sendai virus to red blood cells with good results by using a total site number without considering receptor-mediated attachment. Sendai virus binds sialyloligosaccharide receptors, presumably present in large numbers on a red blood cell and has a maximum number of binding sites that is roughly equivalent to a cell fully covered by virus. Thus, Sendai virus probably binds by mode 3. Because receptors are not appreciably saturated in mode 3, the kinetic equations in the model would simplify to show that attachment could be reasonably described in terms of a reversible, single step as used by Bentz et al. (1988). However, the overall forward and reverse attachment rates in these equations would be nonlinearly dependent on receptor number. Therefore, the present model represents an extension of the attachment portion of previous, "single step" attachment models by predicting how the forward and reverse attachment rates will depend upon the number of receptors present on the cell.

Using simple criteria to establish what mode of binding is used by a virus it has been possible to extract measures of receptor number and affinity from binding data. For Adenovirus 2, the experimentally measured receptor number (6,000/cell) falls within the range of receptor numbers predicted by the model (4,000–15,000/cell). Using the measured receptor number the model predicted an affinity of 2–6 $10^7$ $M^{-1}$ for the Adenovirus 2 receptor, which is within the estimated range of $10^7$–$10^9$ $M^{-1}$.

Using estimates of receptor number and affinity it has been possible to postulate what type of bond is involved and how it relates to pathology of the virus. The results for three broad host range viruses show receptor numbers of $\sim 10^5$/cell or greater and affinities in the range of $10^4$–$10^6$ $M^{-1}$. This range of affinities is typical of a lectin binding reaction which is used by numerous other enveloped viruses and supports the idea that these viruses attach to a highly conserved moiety by multiple, low affinity bonds (Marsh and Helenius, 1989; Marsh, 1984).

Histocompatibility antigens (HA) appear to be involved in Semliki Forest virus binding (Helenius et al., 1978), although cells that do not express these antigens can be infected (Oldstone et al., 1980). The large receptor number, low affinity, and ability of cells not expressing HA to become infected suggests that the virus may bind a moiety that is part of the HA but also present on other cell surface molecules (i.e., an oligosaccharide).

For baculovirus, very little is known about the nature of the VAP/receptor bond. The experiments presented are the first to demonstrate that AcMNPV binding is receptor mediated. The range of affinities and receptor numbers predicted by the model seem to correspond with its broad tissue specificity and host range and give direction to experimentally identifying the VAP/receptor interaction involved. It should be clear that application of the model to an experimental system about which noting was previously known actually yields useful, quantitative information about the mechanism of binding. Therefore, one of the uses of this paper is its ability to interpret data from previously uncharacterized system in terms of real, fundamental parameters.

The amount of binding predicted by the model is very sensitive to receptor density and receptor affinity (results not shown), an effect not observed with monovalent ligand binding. This nonlinear effect on binding is due to the cumulative effect of changing every step in a series of reversible reactions in the same direction. For example, the model predicts that a three-fold reduction in a typical mode 3 affinity ($10^5$ $M^{-1}$) or receptor number ($10^6$) results in a nearly 50-fold decrease in virus affinity for the cell. These sensitivities can begin to explain why point mutations in influenza virus that cause subtle changes in its affinity for different sialic acid linkages can also cause it to change species preference (Paulson et al., 1986; Rogers et al., 1983). Subtle changes in receptor number can also explain how the binding of a broad host range virus to different cells can be so diverse. A large number of cell types probably express the common moiety to which the virus binds but only those cells that contain a critical amount of the moiety will display significant binding of the virus.

For many cases it has been shown that receptor expression is linked to cell infection (Tardieu et al., 1982; Maddon et al., 1986; Morishima et al., 1982). Once the two- and three-dimensional receptor affinities are known it is possible to predict the effects of changes in receptor number on binding and thus, possibly infectivity. Using this model it should be possible to correlate the effect of receptor number on the infectivity of a given virus by measuring binding and infectivity of different cell lines. Experiments of this type, relating AcMNPV/host-cell binding to AcMNPV/host-cell infectivity are currently under way.

It is likely that the choice of the parameter, $P$, will be questioned. $P$ represents a negative cooperativity of binding additional VAPs with cell receptors after a first successful interaction. Such a reduction in probability is believed to be likely because the geometry of the viral/cell interface precludes straightforward VAP/receptor interactions. Either the virus must rotate to bring additional VAPs within the reaction plane of the cell surface, or the

cell membrane must be sufficiently folded in the interfacial region to allow direct contact between potentially reacting partners. Also, $P$ likely includes other effects such as steric hindrance and access of additional receptors to the interfacial region. In the Appendix, an initial attempt is made to justify such a reduced probability of additional binding; indeed, much more sophisticated treatments can be imagined, such as the Crothers and Metzger (1972) model which shows how the second binding site of an antibody might show reduced affinity corresponds to the first. More sophisticated treatments such as this usually reduce to a simple probability of interaction, so that the use of the lumped parameter, $P$, seems justified. Furthermore, it should be noted that binding experiments are typically performed at 4°C to reduce internalization (all of the data presented here were obtained at 4°C). Because $P$ likely depends on the shape of the interface between the virus and cell and because thermal undulations will necessarily be temperature dependent, $P$ is likely to be a function of temperature.

In summary, three modes of virus attachment have been proposed that can explain the diverse virus binding characteristics observed in literature. Simple criteria can be used to establish which mode is used for a given virus/cell system. A model was proposed that accounts for receptor-mediated attachment, nonspecific virus/cell and virus/virus binding and spatial factors that can be involved in virus attachment. The model can describe each mode in different limits and can be applied to virus binding data to extract key physical information such as receptor number and affinity. These values can be used to postulate the type of VAP/receptor interaction involved and to predict binding at different parameter values.

## APPENDIX

## A-1. Subtraction of nonspecific binding

Nonspecific binding between the cell and virus is determined by measuring the difference in binding of labeled virus in the presence and absence of excess unlabeled virus. However, this measurement can include both nonspecific virus/cell and virus/virus binding. By this method it is not possible to know to what extent each occurs. Often times, nonspecific binding is subtracted from the total binding to give an apparent specific binding. If this quantity is large, subtracting it changes the appearance of the binding curve dramatically and can make mode 3 binding appear as mode 2 as demonstrated in Fig. A-1 for the binding of VSV to Vero cells (Schlegel et al., 1982). The maximum number of viruses that a cell can bind is shown by the intersection of the solid line with the bound axis. When the nonspecific binding is subtracted, the number of apparent sites becomes ~5,000, as shown by the dashed line, which has no physical meaning according to mode 3. Virus/virus binding must almost certainly be occurring because the level of the measured nonspecific binding continues past the point at which the cell is completely covered.

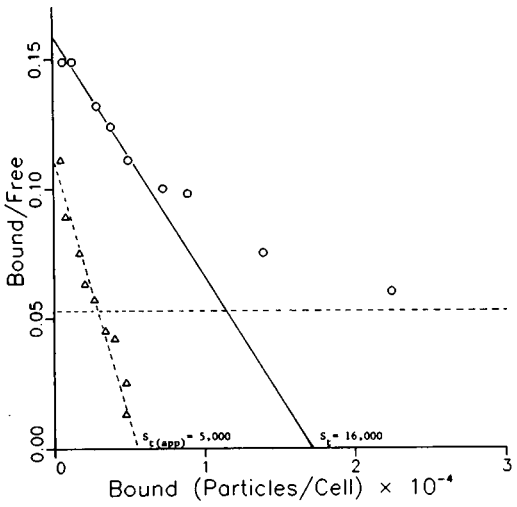


FIGURE A-1 The Scatchard plot for the published binding data of Vesicular Stomatitis virus attaching to Vero cells (Schlegel et al., 1982). The specific and nonspecific binding were both measured. The lower curve shows the model fit to the specific binding data (*triangles*) and the upper curve shows the model fit to the total binding data (*open circles*) which includes virus-cell nonspecific binding, but does not include virus-virus binding.

## A-2. Estimation of the factor, $P$

The parameter, $P$, in the model is a lumped parameter that includes factors that will influence the forward and reverse two-dimensional reaction rates. Using $s/D_{(max)1}$, as shown in Fig. 3 as an estimate of $P$ shows that $P$ is ~0.1 for Semliki Forest virus, assuming the value of $s$ to be 1 nm. This is the upper limit assumed for the other enveloped viruses. For Adenovirus, the angle between the nearest neighbors is much larger so that the upper limit on $P$ is ~0.03 or smaller.

## A-3. Estimation of the number of available VAPs at the surface, $N$

The same types of calculations in A-2 can be used to show how $P$ will vary as a function of the distance of a VAP from the nearest bond. Assuming equidistant spacing of VAPs on a virus the angle between any two VAPs can be calculated. After a virus binds one receptor it then has a ring of six nearest neighbors, each with an equal probability to react. The next ring, at roughly twice angle of the first, has a much smaller probability of reacting based just on its probability of being in the proper plane. Fig. 3 shows that for the second ring, $D_{(max)2}$ does not intersect the plane of reaction. Orientation and strain on a bond that would form would tend to make the difference between the factor, $P$, for each ring even larger. Thus, with the exception of adenovirus, all other viruses were assumed to have a value for $N$ of 7 which is the sum of the initial bond and its nearest number of neighbors.

## A-4. Experimental protocol used for AcMNPV binding experiments

### Cells

*Spodoptera frugiperda*-9 (Sf-9), *Spodoptera frugiperda*-21, *Trichoplusia ni*-368, *Trichoplusia ni* 5b1-4, and two uncharacterized

midgut fatbody *Trichoplusia ni* cell lines were used in the binding studies. Only the results for Sf-9 are reported. All cell lines were maintained in T-flasks (Corning) at 26° C in TNMFH medium plus 10% Fetal Bovine Serum (Gibco Laboratories, Grand Island, NY).

## Virus

Unlabeled Ac-1 *Autographa californica* Multiple Nuclear Polyhedrosis virus was grown by inoculating nearly confluent Sf-21 cells in T-flasks with Ac-1 at a multiplicity of infection of 10 for 1 h. The inoculum was then removed and replaced by fresh media. The virus-containing media was removed after 48 h and spun at 5,000 *g* to remove cells and cell debris. The supernatant was spun again under the same conditions. The virus in the second supernatant were then pelleted by spinning at 35,000 *g* for 1 h through a 34% sucrose cushion. The virus pellet was resuspended in Graces medium (Gibco Laboratories), at pH 6.8 overnight. $^{32}P$-labeled virus was grown by infecting cells in phosphate-free media plus 100 mCi/ml of [$^{32}$P] orthophosphate (DuPont Co., Wilmington, DE). A 1:10 ratio of phosphate containing media was added 24 h post-infection so that cells would produce sufficient quantities of virus. The virus was then harvested and purified in the same way as unlabeled virus. Virus concentration was determined by digesting a known volume of the virus preparation with proteinase K (Boehringer-Manheim) at 2 mg/ml overnight and measuring the released DNA concentration using a TKO 100 fluorometer. The DNA concentration could be directly converted to a virus particle concentration using the molecular weight of AcMNPV DNA.

## Binding experiments

One day previous to the experiment, cells were added at 80% confluency to Falcon 24-multiwell plates. These were then allowed to firmly attach and grow to confluency overnight. The next day the media in each well was successively removed and replaced by 0.2 ml of Graces media (pH 6.8) at 4° C containing a known virus concentration and activity. The cells and virus were then incubated together at 4° C for 18 h to come to equilibrium. After the incubation, the media was removed and the cells were then washed once to remove any remaining, unbound virus. The cell layer was then thoroughly removed by successive scraping and washing so that the bound virus activity could be measured in a scintillation counter to determine the number of bound viruses per well. Cell number per well was separately measured in a control plate by gently pipetting off the cells and counting in a hemocytometer.

The author would like to thank Mike Graham for assistance in obtaining the numerical methods and Lyn Gallo for her assistance in maintaining the cells lines used in the binding experiments.

We gratefully acknowledge support from the National Science Foundation (NSF EET-8807089). This work was also supported in part by a grant from the Cornell Biotechnology Program which is sponsored by the New York State Science and Technology Foundation, a consortium of industries, the U. S. Army Research Office, and the National Science Foundation. This support was in the form of a predoctoral fellowship to T. J. Wickham.

*Received for publication 11 August 1989 and in final form 20 June 1990.*

## REFERENCES

Alcami, A., A. L. Carrascosa, and E. Vinuela. 1989. Saturable binding sites mediate the entry of African Swine Fever virus into VERO cells. *Virology.* 168:393–398.

Allaway, G. P., I. U. Pardoe, A. Tavakkol, and A. T. H. Burness. 1986. Encephalomyocarditis virus attachment. *In* Virus Attachment and Entry into Cells. *Proc. Am. Soc. Microbiol. Conf., Philadelphia PA.* R. L. Crowell and K. Lonberg-Holm, editors. 116–125.

Baxt, B., and D. O. Morgan. 1986. Nature of the interaction between foot-and-mouth disease virus and cultured cells. *In* Virus Attachment and Entry into Cells. *Proc. Am. Soc. Microbiol. Conf., Philadelphia, PA.* R. L. Crowell and K. Lonberg-Holm, editors. 126–137.

Bell, G. I. 1978. Models for the specific adhesion of cells to cells. *Science (Wash. DC).* 200:618–627.

Bentz, J., S. Nir, and D. G. Covell. 1988. Mass action kinetics of virus-cell aggregation and fusion. *Biophys. J.* 54:449–462.

Boldt, D. H., and R. D. Lyons. 1979. Fractionation of human lymphocytes with plant lectins. I. Structural and functional characteristics of lymphocytes subclasses isolated by an affinity technique using lens culinaris lectin. *Cell. Immunol.* 48:82.

Brendel, V., and A. S. Perelson. 1987. Kinetic analysis of adsorption processes. *SIAM (Soc. Ind. Appl. Math.) J.* 47:1306–1319.

Bukrinskaya, A. G. 1982. Penetration of viral genetic material into host cell. *Adv. Virus Res.* 27:141–204.

Burness, A. T. H. 1981. Glycophorin and sialylated components as receptors for viruses. *In* Receptors and Recognition. Virus Receptors, Part 2. K. Lonberg-Holm and L. Philipson, editors. Chapman and Hall, London. 8:65–84.

Cahan, L. D., R. Singh, and J. C. Paulson. 1983. Sialyloligosaccharide receptors of binding variants of polyoma virus. *Virology.* 130:281–289.

Co, M. S., G. N. Gaulton, J. Liu, B. N. Fields, and M. I. Greene. 1986. Structural characterization of the mammalian Reovirus receptor. *In* Virus Attachment and Entry into Cells. *Proc. Am. Soc. Microbiol. Conf., Philadelphia, PA.* R. L. Crowell and K. Lonberg-Holm, editors. 138–143.

Colonno, R. J., J. H. Condra, S. Mizutani, P. L. Callahan, M. E. Davies, and M. A. Murcko. 1988. Evidence for the direct involvement of the rhinovirus canyon in receptor binding. *Proc. Natl. Acad. Sci. USA.* 85:5449–5453.

Crothers, D. M., and H. Metzger. 1972. The influence of polyvalency on the binding properties of antibodies. *Immunochemistry.* 9:341–357.

Dalgleish, A. G., P. C. L. Beverly, P. R. Clapham, D. H. Crawford, M. F. Greaves, and R. A. Weiss. 1984. The CD4 (T4) antigen is an essential component of the receptor for the AIDS retrovirus. *Nature (Lond.).* 312:763–767.

DeLisi, C. 1980*a*. The biophysics of ligand-receptor interactions. *Q. Rev. Biophys.* 13:201–230.

DeLisi, C. 1980*b*. Theory of clustering of cell surface receptors by ligands of arbitrary valence: dependence of dose response patterns on a coarse cluster characteristic. *Math. Biosci.* 52:159–184.

Eigen, M. 1974. Diffusion control in biochemical reactions. *In* Quantum Statistical Mechanics in the Natural Sciences. S. L. Minz and S. M. Wiedermayer, editors. Plenum Publishing Corporation, New York. 37–61.

Epstein, R. L., M. L. Powers, R. B. Rogart, and H. L. Weiner. 1984. Binding of $^{125}$I-labelled Reovirus to cell surface receptors. *Virology.* 133:46–55.

Fries, E., and A. Helenius. 1979. Binding of Semliki Forest virus and its spike glycoproteins to cells. *Eur. J. Biochem.* 97:213–220.

Gandolfi, A., M. A. Giovenco, and R. Strom. 1978. Reversible binding of multivalent antigen in the control of B lymphocyte activation. *J. Theor. Biol.* 74:513–521.

Haywood, A. M. 1974. Characteristics of Sendai virus in a model membrane. *J. Mol. Biol.* 83:427–436.

Helenius, A., and M. Marsh. 1982. Endocytosis of enveloped animal viruses. *In* Membrane Recycling. Pitman Books, Ltd., London. (Ciba Foundation Symposium 92). 59–76.

Helenius, A., B. Morin, E. Fries, K. Simmons, P. Robinson, V. Schirrmacher, C. Terhorst, and J. L. Strominger. 1978. Human (HLA-A and HLA-B) and murine (H-2K and H-2D) histocompatibility antigens are cell surface receptors for Semliki Forest virus. *Proc. Natl. Acad. Sci. USA.* 75:3846–3850.

Hertz, C. M., D. J. Graves, D. A. Lauffenburger, and F. T. Serota. 1985. Use of cell affinity chromotography for separation of lymphocyte subpopulations. *Biotech. Bioeng.* 27:603–612.

Hindmarsh, A. C. 1983. ODEpack, a systemized collection of ODE solvers. *In* Scientific Computing. R. S. Steplemen et al., editors. North-Holland, Amsterdam. 55–64.

Klatzman, D., E. Champagne, S. Chamaret, J. Gruest, D. Geutard, T. Hercend, J.-C. Gluckman, and L. Montagnier. 1984. T-lymphocyte T4 molecule behaves as the receptor for human retrovirus LAV. *Nature* (*Lond.*). 312:767–771.

Kuroda, K., K. Kawasaki, and S. Ohnishi. 1985. Characterization of the fusogenic properties of Sendai virus: kinetics of fusion with erythrocyte membranes. *Biochemistry.* 24:4739–4745.

Lamarre, D., A. Ashkenazi, S. Fleury, D. H. Smith, R. P. Sekaly, and D. J. Capon. 1989. The MHC-binding and gp120-binding functions of CD4 are separable. *Science* (*Wash. DC*). 245:743–746.

Lentz, T. L., T. G. Burrage, A. L. Smith, J. Crick, and G. H. Tignor. 1982. Is the acetylcholine receptor a rabies virus receptor? *Science* (*Wash. DC*). 215:182–184.

Lipkind, M., and V. Urbakh. 1988. Dependence of virus adsorption to the cell surface on the input multiplicity of infection. *Zentralbl. Bakteriol. Mikrobiol. Hyg. 1 Abt. Orig. A.* 269:501–505.

Macken, C. A., and A. S. Perelson. 1982. Aggregation of cell surface receptors by multivalent ligands. *J. Math. Biology.* 14:365–370.

Maddon, P. J., A. G. Dalgleish, J. S. McDougal, P. R. Clapham, R. A. Weiss, and R. Axel. 1986. The T4 gene encodes the AIDS virus receptor and is expressed in the immune system and in the brain. *Cell.* 47:333–348.

Marsh, M. 1984. The entry of enveloped viruses into cells by endocytosis. *Biochem. J.* 218:1–10.

Marsh, M., and A. Helenius. 1989. Virus entry into animal cells. *Adv. Virus Res.* 36:107–151.

Morishima, T., P. R. McClintock, L. L. Billups, and A. L. Notkins. 1982. Expression and modulation of virus receptors on lymphoid and myeloid cells: relationship to infectivity. *Virology.* 116:605–618.

Nemerow, G. R., M. F. E. Siaw, and N. R. Cooper. 1986. Biological significance of the Epstein-Barr virus receptor on B lymphocytes. *In* Virus Attachment and Entry into Cells. *Proc. Am. Soc. Microbiol. Conf., Philadelphia, PA.* R. L. Crowell and K. Lonberg-Holm, editors. 160–167.

Nir, S., K. Klappe, and D. Hoekstra. 1986. Mass action analysis of kinetics and extent of fusion between Sendai virus and phospholipid vesicles. *Biochemistry.* 25:8261–8266.

Oldstone, M. B. A., A. Tishon, F. Dutko, S. I. T. Kennedy, J. J. Holland, and P. W. Lampert. 1980. Does the major histocompatibility complex serve as a specific receptor for Semliki Forest virus? *J. Virol.* 34:256–265.

Paulson, J. C., J. E. Sadler, and R. L. Hill. 1979. Restoration of specific myxovirus receptors to asialoerythrocytes by incorporation of sialic acid with pure sialyltransferases. *J. Biol. Chem.* 254:2120–2124.

Paulson, J. C., G. N. Rogers, J.-I. Murayama, G. Sze, and E. Martin. 1986. Biological implications of influenza virus receptor specificity. *In* Virus Attachment and Entry into Cells. *Proc. Am. Soc. Microbiol. Conf., Philadelphia, PA.* R. L. Crowell and K. Lonberg-Holm, editors. 144–151.

Perelson, A. S. 1981. Receptor clustering on a cell surface. III. Theory of receptor crosslinking by multivalent ligands: description by ligand states. *Math. Biosci.* 53:1–39.

Perelson, A. S. 1985. A model for antibody mediated cell aggregation: rosette formation. *In* Mathematics and Computers in Biomedical Applications. J. Eisenfeld and C. DeLisi, editors. Elsevier Science Publications, North Holland/New York 31–37.

Perelson, A. S., and C. DeLisi. 1980. Receptor clustering on a cell surface. I. Theory of receptor cross-linking by ligands bearing two chemically identical functional groups. *Math. Biosci.* 48:71–110.

Persson, R., U. Svensson, and E. Everitt. 1983. Virus-receptor interaction in the adenovirus system. II. Capping and cooperative binding of virions on HeLa cells. *J. Virol.* 46:956–963.

Philipson, L., K. Lonberg-Holm, and U. Pettersson. 1968. Virus-receptor interaction in an adenovirus system. *J. Virol.* 2:1064–1075.

Press, W. H., B. P. Flannery, S. A. Teukolsky, and W. T. Vetterling. 1983. Numercial Recipes. Cambridge University Press, New York. 274–282.

Rogers, G. N., J. C. Paulson, R. S. Daniels, J. J. Skehel, I. A. Wilson, and D. C. Wiley. 1983. Single amino acid substitutions in influenza haemagglutinin change receptor binding specificity. *Nature* (*Lond.*). 304:76–78.

Schlegel, R., M. C. Willingham, and I. H. Pastan. 1982. Saturable binding sites for Vesicular Stomatitis virus on the surface of Vero cells. *J. Virol.* 43:871–875.

Smoluchowski, M. V. 1917. Versuch einer mathematischen theorie der koagulationskinetik kolloider losungen. *Z. Phys. Chem.* 82:129–168.

Svensson, U. 1985. Role of vesicles during Adenovirus 2 internalization into HeLa cells. *J. Virol.* 55:442–449.

Tardieu, M., R. L. Epstein, and H. L. Weiner. 1982. Interaction of viruses with cell surface receptors. *Int. Rev. Cytol.* 80:27–61.

Taylor, H. P., and N. R. Cooper. 1989. Human Cytomegalovirus binding to fibroblasts is receptor mediated. *J. Virol.* 63:3991–3998.

Thimmig, R. L., J. V. Hughes, R. J. Kinders, A. G. Milenkovic, and T. C. Johnson. 1980. Isolation of the glycoprotein of Vesicular Stomatitis virus and its binding to cell surfaces. *J. Gen. Virol.* 50:279–291.

Tsao, Y-S., and L. Huang. 1986. Kinetic studies of Sendai virus-target membrane interaction. Independent analysis of binding and fusion. *Biochemistry.* 25:3971–3976.

Volkman, L. E. 1986. The 64K envelope protein of budded *Autographa californica* Nuclear Polyhedrosis virus. *In* Current Topics in Microbiology and Immunology. Springer-Verlag, Berlin Heidelberg. 131:103–118.

Weis, W., J. H. Brown, S. Cusack, J. C. Paulson, J. J. Skehel, and D. C. Wiley. 1988. Structure of the influenza virus haemagglutinin complexed with its receptor, sialic acid. *Nature* (*Lond.*). 333:426–431.

White, J. M., and D. R. Littman. 1989. Viral receptors of the immunoglobin superfamily. *Cell.* 56:725–728.

Wunner, W. H., K. J. Reagan, and H. Koprowski. 1984. Characterization of saturable binding sites for Rabies virus. *J. Virol.* 50:691–697.

Yamada, S., and S. Ohnishi. 1986. Vesicular Stomatitis virus binds and fuses with phospholipid domain in target cell membranes. *Biochemistry.* 25:3703–3708.